JOURNAL OF COMPUTATIONAL PHYSICS 35, 206–228 (1980)

Truncation Error Terms in the Kinetic Energy Calculation in the HELP Algorithm and Their Consequences

JAMES A. SCHMITT

U.S. Army Armament Research and Development Command
Ballistic Research Laboratory, Aberdeen Proving Ground, Maryland 21005

Received October 20, 1978

When the HELP computer code is applied to conical-shaped charge warhead problems, the computed internal energy predicts a thermal state completely different than that indicated by experiments. The cause of this phenomenon is the numerical interchange of the kinetic energy to internal energy which is generated by terms of the order of the truncation error in the kinetic energy calculation. A correction is given and qualitative thermal agreement is achieved for the first time between a HELP calculation and experimental evidence. The effects of the original kinetic energy calculation on the accuracy of the internal energy is problem dependent and criteria for such a determination are given in terms of the truncation error terms for the internal energy. A mesh refinement study further illustrates the consequences of the original and modified kinetic energy calculations. The same phenomenon can occur in other computer codes with a Particle-In-Cell based algorithm and the given correction is applicable.

I. INTRODUCTION

Time-dependent two-dimensional Eulerian computer codes like HELP [1] and HULL [2] are utilized to describe the unsteady interactions of continuous media (fluid and/or solids). Many of these continuum codes have a common ancestorial algorithm, the Particle-In-Cell method [3–5]. During the evolutionary process, the new codes have deviated substantially from the original PIC method; for example, the discrete particles were replaced by a continuum, certain Lagrangian-type features were abandoned, and for calculations in solid mechanics, material strength and effects of the deviatoric stress tensor were included. These codes can produce very successful simulations but often the results are not totally satisfactory. Such is the case with the HELP code which is used by several research laboratories and corporations for diverse applications in compressible flow and elastic–plastic flows. In certain ballistics applications at the U.S. Army Ballistics Research Laboratory, the code predicts velocities satisfactorily but an internal energy which implies a different thermal state than that indicated by experimental evidence. The purpose of this paper is to show that the original approximations in HELP lead to specific error terms that significantly and consistently influence the internal energy calculation and to propose a correction within the context of the current algorithm.

0021-9991/80/050206–23$02.00/0

The internal energy algorithm in HELP is based on the finite-difference approximation of the total energy equation and the kinetic energy calculated from updated mass and momentum values. This internal energy approximation is shown to include terms of the order of the truncation error which arise in the kinetic energy calculation from the finite-difference approximations of the mass and momentum equations. These terms, in certain cases, cause a less accurate calculation of the internal energy (they increase the truncation error) and produce an interchange of energy at each phase which is not modeled in the governing equations. Evans and Harlow [3] identified an energy transfer mechanism in the convection phase of the original PIC method which can be seen in HELP. This mechanism is due only to spatial descretization and was illustrated in one dimension. The following analysis involves all the phases in the HELP algorithm, is two dimensional, includes the effect of time discretization, and applies to a different code with a different energy formulation (the PIC algorithm transports total energy but directly calculates the internal energy in its other phases). Although this paper deals exclusively with the HELP algorithm, the concepts and results discussed are applicable to other codes. In particular, the same internal energy phenomenon is seen in calculations performed with the HULL code.

In Section II, the governing equations which are modeled by the HELP algorithm are listed, the corresponding approximations are derived, and other salient features of the algorithm are discussed. Truncation error analyses of the kinetic energy and internal energy calculations in Section III reveal the specific error terms arising from the HELP's finite-difference approximations of the governing equations. Corrections to the algorithm are then proposed. Numerical examples contrasting the original and modified algorithms are discussed in Section IV. Section V contains a summary.

II. The HELP Code

The unsteady motion and interaction of continuous media can be described by a continuity equation, equations of motion, a total energy equation, and an equation of state. For simplicity, we shall consider the Cartesian formulation. The appropriate two-dimensional equations in conservative form are:

$$\frac{\partial \rho}{\partial t} = -\frac{\partial}{\partial x}(\rho u) - \frac{\partial}{\partial y}(\rho v), \tag{1}$$

$$\frac{\partial(\rho u)}{\partial t} = -\frac{\partial}{\partial x}(\rho uu) - \frac{\partial}{\partial y}(\rho vu) - \frac{\partial P}{\partial x} + \frac{\partial}{\partial x}(S_{xx}) + \frac{\partial}{\partial y}(S_{xy}), \tag{2}$$

$$\frac{\partial(\rho v)}{\partial t} = -\frac{\partial}{\partial x}(\rho uv) - \frac{\partial}{\partial y}(\rho vv) - \frac{\partial P}{\partial y} + \frac{\partial}{\partial x}(S_{xy}) + \frac{\partial}{\partial y}(S_{yy}), \tag{3}$$

$$\frac{\partial(\rho E)}{\partial t} = -\frac{\partial}{\partial x}(\rho uE) - \frac{\partial}{\partial y}(\rho vE) - \frac{\partial(uP)}{\partial x} - \frac{\partial(vP)}{\partial y} + \frac{\partial}{\partial x}(S_{xx}u + S_{xy}v) + \frac{\partial}{\partial y}(S_{yy}v + S_{xy}u), \tag{4}$$

where t, x, y, ρ, u, v, P, S_{xx}, S_{yy}, S_{xy}, and E denote the time, two spatial coordinates, density, x and y components of velocity, pressure, the two normal and one shear stress components of the stress deviator tensor, and specific total energy, respectively. The elements of the stress deviator tensor are functions of the velocity gradient. The pressure is computed via an equation of state of the functional form $P = P(\rho, I)$, where I is the specific internal energy. The specific internal energy is obtained as the difference of the specific total energy and the specific kinetic energy:

$$I = E - 0.5(u^2 + v^2). \tag{5}$$

If the conservation Eqs. (1–4) are integrated over an arbitrary control area, the time rate of change of a quantity within the control area can be related to the integrals of other quantities over the boundary enclosing that area. Performing the integration and using Green's theorem, we obtain

$$\frac{\partial}{\partial t}\int_A \rho\, dA = \int_B (\rho v\, dx - \rho u\, dy), \tag{6}$$

$$\frac{\partial}{\partial t}\int_A \rho u\, dA = \int_B u(\rho v\, dx - \rho u\, dy) - \int_B P\, dy + \int_B (S_{xx}\, dy - S_{xy}\, dx), \tag{7}$$

$$\frac{\partial}{\partial t}\int_A \rho v\, dA = \int_B v(\rho v\, dx - \rho u\, dy) + \int_B P\, dx + \int_B (S_{xy}\, dy - S_{yy}\, dx), \tag{8}$$

$$\frac{\partial}{\partial t}\int_A \rho E\, dA = \int_B E(\rho v\, dx - \rho u\, dy) + \int_B (Pv\, dx - Pu\, dy) + \int_B [(S_{xx}u + S_{xy}v)\, dy - (S_{yy}v + S_{xy}u)\, dx], \tag{9}$$

where B is the boundary of area A in the positive sense. Equation (7), for example, equates the time rate of change of the x-component of the momentum within the area A to the product of the specific momentum in the x direction and the net mass flow into the area plus the sum of certain surface forces (the pressure and the x-components of the deviator stress tensor) exerted over the boundary enclosing the area. Such interpretations are used to determine the HELP approximations to the governing equations.

The HELP code is an Eulerian code capable of describing unsteady multimaterial interaction and of treating material strength as an elastic–plastic phenomenon. A consequence of the multimaterial capability is mixed cells (cells containing more than one material). The complex treatment of these cells is important and indispensable to the correct running of the code. However, an accurate and complete analysis of these numerical techniques is unwieldy. An analysis of the pure cell (a cell containing only one material) algorithm reveals the cause of the internal energy problem. Hence, the following discussion will address only the pure cell algorithm. Furthermore, we consider only interior cells. We assume that the grid spacing Δx in the x-direction is constant as well as Δy in the y-direction. The control area A is taken to be the ith, jth

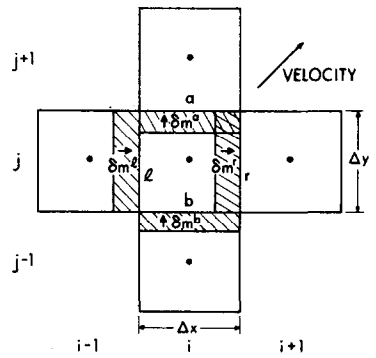

FIG. 1. Computational cell for Cartesian formulation of HELP.

computational cell. See Fig. 1. The left, right, top, and bottom boundaries of this cell are denoted by the letters l, r, a, and b, respectively. A time step Δt in this explicit algorithm is determined by a Courant condition. The area integrals in Eqs. (6)–(9) are approximated by $m = \rho \Delta x \Delta y$, mu, mv, and mE, respectively, where m denotes the mass per unit length. All the values are at the center of the computational cell. The time derivatives are approximated by a forward difference. The values of the cell centered mass, momentum, and specific total energy at the new time level are found from the values at the previous time level. This is accomplished in three stages by determining the time rate of change of the mass, momentum, and total energy due to (i) the effects of the deviatoric stresses, (ii) the effects of the pressure, and (iii) the effects of the convection terms. These phases are appropriately named SPHASE, HPHASE, and TPHASE, respectively. During each time step, each value of the mass, momentum, and total energy is updated sequentially by each phase in the order listed and each phase uses the previously updated values as its initial values. Each phase is solved independently of the others and are interconnected only through the initial values. The boundary integrals in Eqs. (6)–(9) are approximated using the current values of the integrands at the boundaries of the computational cell. The pressure is calculated before SPHASE and the stress deviator tensor is updated at the beginning of SPHASE. The internal energy is updated by Eq. (5) at the end of each phase.

Specifically, we list the HELP approximations to the conservation of mass, momentum, and total energy equations. The HELP approximations to the Eqs. (6)–(9) in the SPHASE portion of the calculation for the ith, jth cell at the nth time step are:

$$\tilde{m} = m, \tag{10}$$

$$\widetilde{mu} = mu + (S_{xx}^{\,r} - S_{xx}^{\,l})\,\Delta y\,\Delta t + (S_{xy}^{\,a} - S_{xy}^{\,b})\,\Delta x\,\Delta t, \tag{11}$$

$$\widetilde{mv} = mv + (S_{xy}^{\,r} - S_{xy}^{\,l})\,\Delta y\,\Delta t + (S_{yy}^{\,a} - S_{yy}^{\,b})\,\Delta x\,\Delta t, \tag{12}$$

$$\begin{aligned}\widetilde{mE} = mE &+ [(u^r S_{xx}^{\,r} - u^l S_{xx}^{\,l}) + (v^r S_{xy}^{\,r} - v^l S_{xy}^{\,l})]\,\Delta y\,\Delta t \\ &+ [(u^a S_{xy}^{\,a} - u^b S_{xy}^{\,b}) + (v^a S_{yy}^{\,a} - v^b S_{yy}^{\,b})]\,\Delta x\,\Delta t,\end{aligned} \tag{13}$$

where the tilde denotes the SPHASE updated value and the letter superscripts r, l, a, and b refer to the evaluation of the term at the corresponding boundary. A variable without subscripts or superscripts denotes that quantity evaluated at the center of the ith, jth cell at the nth time level. The boundary value of a variable is the average of its cell-centered values adjacent to that boundary, for example, $S^r{}_{xx} = 0.5\,[(S_{xx})^n_{i+1,j} + (S_{xx})^n_{i,j}]$, where $(S_{xx})^n_{i,j} = S_{xx}[(i - \frac{1}{2})\,\Delta x, (j - \frac{1}{2})\,\Delta y, n\Delta t]$. See Fig. 1. The approximations (10)–(13) can be derived from a physical interpretation of the SPHASE portions of Eqs. (6)–(9). For example, consider approximation (13). The effects of the stress deviator tensor on the time rate of change of the total energy $[\widetilde{mE} - mE]/\Delta t$ during the entire time step Δt are governed by the work rates per unit surface area, uS_{xx} and vS_{xy}, acting on the right and left boundaries and vS_{yy} and uS_{xy} on the top and the bottom boundaries, times the length of these boundaries.

The errors that are introduced by the numerical approximation (13) can be obtained by expanding the corresponding finite-difference equation in a Taylor series. We use the mass–density relation $m = \rho\Delta x\Delta y$ and rewrite Eq. (13) as

$$\frac{\widetilde{\rho E} - \rho E}{\Delta t} - \frac{u^r S_{xx}{}^r - u^l S_{xx}{}^l}{\Delta x} - \frac{v^r S_{xy}{}^r - v^l S_{xy}{}^l}{\Delta x} - \frac{u^a S_{xy}{}^a - u^b S_{xy}{}^b}{\Delta y} - \frac{v^a S_{yy}{}^a - v^b S_{yy}{}^b}{\Delta y} = 0. \tag{14}$$

A Taylor series expansion of each dependent variable in Eq. (14) at the center of the ith, jth cell at the nth time level leads to

$$\begin{aligned}
&\frac{\partial(\rho E)}{\partial t} - \frac{\partial}{\partial x}[uS_{xx} + vS_{xy}] - \frac{\partial}{\partial y}[uS_{xy} + vS_{yy}] \\
&\quad = -\Delta t\,\frac{1}{2}\left\{\frac{\partial^2(\rho E)}{\partial t^2}\right\} \\
&\qquad - \Delta x^2\left\{\frac{1}{6}\frac{\partial^3}{\partial x^3}(uS_{xx} + vS_{xy}) - \frac{1}{4}\frac{\partial}{\partial x}\left(\frac{\partial u}{\partial x}\frac{\partial S_{xx}}{\partial x} + \frac{\partial v}{\partial x}\frac{\partial S_{xy}}{\partial x}\right)\right\} \\
&\qquad - \Delta y^2\left\{\frac{1}{6}\frac{\partial^3}{\partial y^3}(uS_{xy} + vS_{yy}) - \frac{1}{4}\frac{\partial}{\partial y}\left(\frac{\partial u}{\partial y}\frac{\partial S_{xy}}{\partial y} + \frac{\partial v}{\partial y}\frac{\partial S_{yy}}{\partial y}\right)\right\} \\
&\qquad + O(\Delta t^2) + O(\Delta x^3) + O(\Delta y^3).
\end{aligned} \tag{15}$$

The terms in Eq. (4) which are relevant to SPHASE are given on the left-hand side of Eq. (15) and the dominant error terms appear on the right-hand side. The order of error terms are $O(\Delta t)$, $O(\Delta x^2)$, and $O(\Delta y^2)$. Thus, approximation (13) is first order in time and second order in space within the context of SPHASE (assuming the post SPHASE values are those at the end of the time step). A similar analysis and results hold for approximations (11) and (12), and Eqs. (2) and (3), respectively.

The HPHASE approximations are

$$\overline{m} = m, \tag{16}$$

$$\overline{mu} = m\tilde{u} - (P^r - P^l)\,\Delta y\,\Delta t, \tag{17}$$

$$\overline{mv} = m\tilde{v} - (P^a - P^b)\,\Delta x\,\Delta t, \tag{18}$$

$$\overline{mE} = m\tilde{E} - (P^r\tilde{u}^r - P^l\tilde{u}^l)\,\Delta y\,\Delta t - (P^a\tilde{v}^a - P^b\tilde{v}^b)\,\Delta x\,\Delta t, \tag{19}$$

where the bar denotes the HPHASE updated value and $P = P(\rho, I)$. The truncation error analysis of approximation (19) can be made in exactly the same manner as for approximation (13). The result is

$$\begin{aligned}\frac{\partial(\widetilde{\rho E})}{\partial t} + \frac{\partial(P\tilde{u})}{\partial x} + \frac{\partial(P\tilde{v})}{\partial y} &= -\Delta t\left\{\frac{1}{2}\frac{\partial^2(\widetilde{\rho E})}{\partial t^2}\right\} - \Delta x^2\left\{\frac{1}{6}\frac{\partial^3(P\tilde{u})}{\partial x^3} - \frac{1}{4}\frac{\partial}{\partial x}\left(\frac{\partial\tilde{u}}{\partial x}\frac{\partial P}{\partial x}\right)\right\} \\ &\quad - \Delta y^2\left\{\frac{1}{6}\frac{\partial^3(P\tilde{v})}{\partial y^3} - \frac{1}{4}\frac{\partial}{\partial y}\left(\frac{\partial\tilde{v}}{\partial y}\frac{\partial P}{\partial y}\right)\right\} \\ &\quad + O(\Delta t^2) + O(\Delta x^3) + O(\Delta y^3).\end{aligned} \tag{20}$$

Thus Eq. (19) is a first-order approximation in time and second order in space within the context of HPHASE. The other HPHASE approximations (17) and (18) are of the same order.

For simplicity in the discussion of the TPHASE approximations, we assume that the velocity has both positive x- and y-components. The TPHASE approximations which model the convection between cells are:

$$m^{n+1} = m + \delta m^l - \delta m^r + \delta m^b - \delta m^a, \tag{21}$$

$$(mu)^{n+1} = m\bar{u} + \delta m^l\bar{u}_{i-1,j} - \delta m^r\bar{u} + \delta m^b\bar{u}_{i,j-1} - \delta m^a\bar{u}, \tag{22}$$

$$(mv)^{n+1} = m\bar{v} + \delta m^l\bar{v}_{i-1,j} - \delta m^r\bar{v} + \delta m^b\bar{v}_{i,j-1} - \delta m^a\bar{v}, \tag{23}$$

$$(mE)^{n+1} = m\bar{E} + \delta m^l\bar{E}_{i-1,j} - \delta m^r\bar{E} + \delta m^b\bar{E}_{i,j-1} - \delta m^a\bar{E}, \tag{24}$$

where δm^l, δm^b, δm^r, and δm^a denote the convected mass per unit length from the left and bottom cells and to the right and top cells, respectively. See Fig. 1. In general, $\delta m^d = \rho^d L^d\bar{u}^d\Delta t$, where ρ^d denotes the density of the cell from which the mass is transported, $\bar{u}^d$ is the interpolated value of the velocity component normal to the cell boundary and L^d is the length of the cell boundary through which the mass is moved. For example, the factors in δm^l are $\rho^l = \rho_{i-1,j}$, $\bar{u}^l = 0.5\,(\bar{u} + \bar{u}_{i-1,j})/[1 + \Delta t(\bar{u} - \bar{u}_{i-1,j})/\Delta x]$, and $L^l = \Delta y$. We note that $\bar{u}^d$ represents the transport velocity of δm^d based on linear approximations over the time step Δt. The intuitive explanation of the TPHASE approximations for Eq. (21) is that the mass at the end of TPHASE (the

final value at $(n + 1)$ time level) is the mass originally in the cell plus the mass transported into the cell $(\delta m^l, \delta m^b)$ minus the mass transported from the cell $(\delta m^r, \delta m^a)$. For the total energy approximation (24), a similar situation exists, except that now each convected mass is associated with the specific total energy of its "donor" cell. Within the context of TPHASE (assuming the post-HPHASE values are the initial values at the nth time level), approximations (21)–(24) can be shown to be first order in time and space to the TPHASE portions of Eqs. (1)–(4), respectively. For example, to determine the order of approximation (24), we substitute the appropriate mass approximations and obtain

$$\frac{(\rho E)^{n+1} - (\rho \bar{E})}{\Delta t} + \frac{(\rho \bar{E})\,\bar{u}^r - (\rho_{i-1,j}\bar{E}_{i-1,j})\,\bar{u}^l}{\Delta x} + \frac{(\rho \bar{E})\,\bar{v}^a - (\rho_{i,j-1}\bar{E}_{i,j-1})\,\bar{v}^b}{\Delta y} = 0. \tag{25}$$

A Taylor series expansion of each dependent variable in Eq. (25) at the center of the ith, jth cell at the nth time level leads to

$$\frac{\partial(\overline{\rho E})}{\partial t} + \frac{\partial(\rho \overline{E u})}{\partial x} + \frac{\partial(\rho \overline{E v})}{\partial y} = -\frac{\Delta t}{2}\left[\frac{\partial^2(\rho \bar{E})}{\partial t^2} - 2\frac{\partial}{\partial x}\left(\rho \overline{E u}\,\frac{\partial \bar{u}}{\partial x}\right) - 2\frac{\partial}{\partial y}\left(\rho \overline{E v}\,\frac{\partial \bar{v}}{\partial y}\right)\right] + \frac{\Delta x}{2}\left[\frac{\partial}{\partial x}\left(\bar{u}\,\frac{\partial \rho \bar{E}}{\partial x}\right)\right] + \frac{\Delta y}{2}\left[\frac{\partial}{\partial y}\left(\bar{v}\,\frac{\partial \rho \bar{E}}{\partial y}\right)\right] + O(\Delta t^2) + O(\Delta x^2) + O(\Delta y^2). \tag{26}$$

The terms in Eq. (4) which are relevant to TPHASE are given on the left-hand side of Eq. (26) and the dominant error terms appear on the right-hand side. The spatial gradients in the coefficient of Δt in Eq. (26) are the results of the transport velocities' $\bar{u}^r$, $\bar{u}^l$, $\bar{v}^a$, and $\bar{v}^b$ dependence on Δt. The order of the error terms are $O(\Delta t)$, $O(\Delta x)$, and $O(\Delta y)$. Thus, approximation (24) is first order in both time and space, which establishes the assertion.

We have shown that the SPHASE and HPHASE approximations of Eqs. (1)–(4) are first order in time and second order in space and that the TPHASE approximations are first order in both time and space. Consequently, the order of the spatial approximation in TPHASE is less than that for either SPHASE or HPHASE and first-order error terms will be dominant within the algorithm.

III. The Kinetic Energy and Internal Energy Calculations

In order to determine the cause of the unphysical internal energy values produced by the 1975 HELP code in conical-shaped charge calculations, we must investigate how the total energy approximations are combined with the kinetic energy approximations to produce the internal energy approximations. To this end we list the partial

differential equations for the kinetic and internal energies. The partial differential equation governing kinetic energy can be derived from Eqs. (1)–(3) by the following identity:

$$\frac{\partial}{\partial t}(\rho e) = u\frac{\partial \rho u}{\partial t} + v\frac{\partial \rho v}{\partial t} - \frac{1}{2}(u^2 + v^2)\frac{\partial \rho}{\partial t}, \tag{27}$$

and can be written as

$$\frac{\partial}{\partial t}(\rho e) = -\frac{\partial}{\partial x}(\rho u e) - \frac{\partial}{\partial y}(\rho v e) - u\frac{\partial P}{\partial x} - v\frac{\partial P}{\partial y} + u\left(\frac{\partial S_{xx}}{\partial x} + \frac{\partial S_{xy}}{\partial y}\right) + v\left(\frac{\partial S_{xy}}{\partial x} + \frac{\partial S_{yy}}{\partial y}\right), \tag{28}$$

where $e = 0.5(u^2 + v^2)$. An interpretation of the above manipulation is that given the exact solutions of Eqs. (1)–(3), the derived function e is identical to the exact solution of Eq. (28). We shall show that the HELP approximations do not share this property. The partial differential equation governing internal energy can be obtained by subtracting Eq. (28) from Eq. (4) and by using identity (5):

$$\frac{\partial}{\partial t}(\rho I) = -\frac{\partial}{\partial x}(\rho I u) - \frac{\partial}{\partial y}(\rho I v) - P\frac{\partial u}{\partial x} - P\frac{\partial v}{\partial y} + S_{xx}\frac{\partial u}{\partial x} + S_{xy}\left(\frac{\partial v}{\partial x} + \frac{\partial u}{\partial y}\right) + S_{yy}\frac{\partial v}{\partial y}. \tag{29}$$

In the HELP code, the specific kinetic energy e at the end of each phase is computed via

$$e = 0.5\{[(mu)/m]^2 + [(mv)/m]^2\} \tag{30}$$

using the updated values of the mass and momentum from that phase. By using approximations (10)–(12), (16)–(18), and (21)–(23), Eq. (30) and the expressions for the mass in terms of the density, we can write the formulas used to determine the updated specific kinetic energy at the different phases in terms of the initial values at SPHASE, HPHASE, and TPHASE. The resulting expressions are never explicitly used to calculate the kinetic energy but are numerically equivalent to Eq. (30). The results are:

$$\frac{(\widetilde{\rho e}) - \rho e}{\Delta t} = u\left[\frac{S_{xx}{}^{r} - S_{xx}{}^{l}}{\Delta x} + \frac{S_{xy}{}^{a} - S_{xy}{}^{b}}{\Delta y}\right] + v\left[\frac{S_{xy}{}^{r} - S_{xy}{}^{l}}{\Delta x} + \frac{S_{yy}{}^{a} - S_{yy}{}^{b}}{\Delta y}\right] + \left\{\frac{\Delta t}{2\rho}\left[\left(\frac{S_{xx}{}^{r} - S_{xx}{}^{l}}{\Delta x} + \frac{S_{xy}{}^{a} - S_{xy}{}^{b}}{\Delta y}\right)^2 + \left(\frac{S_{xy}{}^{r} - S_{xy}{}^{l}}{\Delta x} + \frac{S_{yy}{}^{a} - S_{yy}{}^{b}}{\Delta y}\right)^2\right]\right\}, \tag{31}$$

$$\frac{\overline{(\rho e)} - \widetilde{(\rho e)}}{\Delta t} = -\tilde{u}\left[\frac{P^r - P^l}{\Delta x}\right] - \tilde{v}\left[\frac{P^a - P^b}{\Delta y}\right] + \left\{\frac{\Delta t}{2\rho}\left[\left(\frac{P^r - P^l}{\Delta x}\right)^2 + \left(\frac{P^a - P^b}{\Delta y}\right)^2\right]\right\}, \tag{32}$$

$$\begin{aligned}
&\frac{(\rho e)^{n+1} - \overline{(\rho e)}}{\Delta t} \\
&= -\frac{\rho \bar{u}^r \bar{e} - \rho_{i-1,j}\bar{u}^l \bar{e}_{i-1,j}}{\Delta x} - \frac{\rho \bar{v}^a \bar{e} - \rho_{i,j-1}\bar{v}^b \bar{e}_{i,j-1}}{\Delta y} \\
&\quad - \left\{\frac{\rho_{i-1,j}\rho}{2\rho^{n+1}}\bar{u}^l\left[\Delta x - \bar{u}^r \Delta t - \bar{v}^a \Delta t \frac{\Delta x}{\Delta y}\right]\left[\left(\frac{\bar{u} - \bar{u}_{i-1,j}}{\Delta x}\right)^2 + \left(\frac{\bar{v} - \bar{v}_{i-1,j}}{\Delta x}\right)^2\right]\right. \\
&\quad + \frac{\rho_{i,j-1}\rho \bar{v}^b}{2\rho^{n+1}}\left[\Delta y - \bar{v}^a \Delta t - \bar{u}^r \Delta t \frac{\Delta x}{\Delta y}\right]\left[\left(\frac{\bar{u} - \bar{u}_{i,j-1}}{\Delta y}\right)^2 + \left(\frac{\bar{v} - \bar{v}_{i,j-1}}{\Delta y}\right)^2\right] \\
&\quad + \frac{\rho_{i-1,j}\rho_{i,j-1}\bar{v}^b \bar{u}^l}{2\rho^{n+1}}\Delta t \frac{\Delta x}{\Delta y}\left[\left(\frac{\Delta y}{\Delta x}\frac{\bar{u} - \bar{u}_{i,j-1}}{\Delta y} - \frac{\bar{u} - \bar{u}_{i-1,j}}{\Delta x}\right)^2\right. \\
&\quad \left.\left. + \left(\frac{\Delta y}{\Delta x}\frac{\bar{v} - \bar{v}_{i,j-1}}{\Delta y} - \frac{\bar{v} - \bar{v}_{i-1,j}}{\Delta x}\right)^2\right]\right\}.
\end{aligned} \tag{33}$$

A truncation error analysis of Eqs. (31)–(33) reveals significant information about the kinetic energy approximations. Since we have shown that the dominant error terms within the HELP algorithm are of first order, we will not write the higher-order terms. Preceeding in a similar fashion to the truncation error analyses of Section II, we obtain for Eq. (31)

$$\begin{aligned}
&\frac{\partial(\rho e)}{\partial t} - u\left(\frac{\partial S_{xx}}{\partial x} + \frac{\partial S_{xy}}{\partial y}\right) - v\left(\frac{\partial S_{xy}}{\partial x} + \frac{\partial S_{yy}}{\partial y}\right) \\
&\quad = -\frac{\Delta t}{2}\left[\frac{\partial^2(\rho e)}{\partial t^2} - \frac{1}{\rho}\left(\frac{\partial S_{xx}}{\partial x} + \frac{\partial S_{xy}}{\partial y}\right)^2 - \frac{1}{\rho}\left(\frac{\partial S_{xy}}{\partial x} + \frac{\partial S_{yy}}{\partial y}\right)^2\right] \\
&\qquad + O(\Delta t^2) + O(\Delta x^2) + O(\Delta y^2).
\end{aligned} \tag{34}$$

The terms in Eq. (28) which are relevant to SPHASE are given on the left-hand side of Eq. (34) and the dominant error terms appear on the right-hand side. The order of the error terms are $O(\Delta t)$, $O(\Delta x^2)$, and $O(\Delta y^2)$. Thus, approximation (31) is first order in time and second order in space, and the order of this approximation is consistent with the other SPHASE approximations. The terms

$$\frac{\Delta t}{2\rho}\left[\left(\frac{\partial S_{xx}}{\partial x} + \frac{\partial S_{xy}}{\partial y}\right)^2 + \left(\frac{\partial S_{xy}}{\partial x} + \frac{\partial S_{yy}}{\partial y}\right)^2\right]$$

in Eq. (34) are the lowest-order terms of those enclosed by braces in Eq. (31). Thus, the braced terms in Eq. (31) which are included in the kinetic energy approximation in SPHASE are of the order of the truncation error.

An analogous truncation error analyses of Eqs. (32) and (33) gives, for HPHASE,

$$\frac{\partial(\widetilde{\rho e})}{\partial t} + \tilde{u}\frac{\partial P}{\partial x} + \tilde{v}\frac{\partial P}{\partial y} = -\frac{\Delta t}{2}\left\{\frac{\partial^2(\widetilde{\rho e})}{\partial t^2} - \frac{1}{\rho}\left(\frac{\partial P}{\partial x}\right)^2 - \frac{1}{\rho}\left(\frac{\partial P}{\partial y}\right)^2\right\} + O(\Delta t^2) + O(\Delta x^2) + O(\Delta y^2), \tag{35}$$

and for TPHASE

$$\begin{aligned}
&\frac{\partial(\overline{\rho e})}{\partial t} + \frac{\partial}{\partial x}(\overline{\rho e u}) + \frac{\partial}{\partial y}(\overline{\rho e v}) \\
&\quad = +\frac{\Delta x}{2}\left\{\frac{\partial}{\partial x}\left[\bar{u}\frac{\partial(\rho\bar{e})}{\partial x}\right] - \rho\bar{u}\left[\left(\frac{\partial\bar{u}}{\partial x}\right)^2 + \left(\frac{\partial\bar{v}}{\partial x}\right)^2\right]\right\} \\
&\quad\quad + \frac{\Delta y}{2}\left\{\frac{\partial}{\partial y}\left[\bar{v}\frac{\partial(\rho\bar{e})}{\partial y}\right] - \rho\bar{v}\left[\left(\frac{\partial\bar{u}}{\partial y}\right)^2 + \left(\frac{\partial\bar{v}}{\partial y}\right)^2\right]\right\} \\
&\quad\quad - \frac{\Delta t}{2}\left\{\frac{\partial^2(\overline{\rho e})}{\partial t^2} - 2\frac{\partial}{\partial x}\left(\bar{u}\rho\bar{e}\frac{\partial\bar{u}}{\partial x}\right) - 2\frac{\partial}{\partial y}\left(\bar{u}\rho\bar{e}\frac{\partial\bar{v}}{\partial y}\right)\right. \\
&\quad\quad - \rho\bar{u}\left(\bar{u} + \bar{v}\frac{\Delta x}{\Delta y}\right)\left[\left(\frac{\partial\bar{u}}{\partial x}\right)^2 + \left(\frac{\partial\bar{v}}{\partial x}\right)^2\right] - \rho\bar{v}\left(\bar{v} + \bar{u}\frac{\Delta x}{\Delta y}\right)\left[\left(\frac{\partial\bar{u}}{\partial y}\right)^2 + \left(\frac{\partial\bar{v}}{\partial y}\right)^2\right] \\
&\quad\quad \left. + \rho\overline{vu}\frac{\Delta x}{\Delta y}\left[\left(\frac{\Delta y}{\Delta x}\frac{\partial\bar{u}}{\partial y} - \frac{\partial\bar{u}}{\partial x}\right)^2 + \left(\frac{\Delta y}{\Delta x}\frac{\partial\bar{v}}{\partial y} - \frac{\partial\bar{v}}{\partial x}\right)^2\right]\right\}.
\end{aligned} \tag{36}$$

As in SPHASE, the HPHASE kinetic energy approximation is first order in time and second order in space, and includes terms (those enclosed in braces in Eq. (32)) which are of the order of the truncation error. Equation (36) shows that the TPHASE kinetic energy approximation is first order in both time and space. The terms enclosed in braces in Eq. (33) contribute only to the $O(\Delta x)$, $O(\Delta y)$, $O(\Delta t)$, and higher-order terms in Eq. (36) and, consequently, are of the order of the truncation error.

Thus, the order of approximations (31)–(33) are in accord with the other approximations in the three phases but these approximations include terms which are of the order of the truncation error: terms of order Δt in SPHASE and HPHASE and order Δt, Δx, and Δy in TPHASE. These terms are consequences of calculating the kinetic energy from Eq. (30) and from the particular choices made in the finite-difference approximations of the mass and momentum equations in each phase. Furthermore, these terms do not model any term of the kinetic energy equation. In fact, if one would write directly a finite-difference approximation to Eq. (28) in a consistent manner with the HELP approximations of Eqs. (1)–(4), the result would be Eqs. (31)–(33) without the braced terms. Thus, the kinetic energy finite-difference solutions within HELP do not share the corresponding property possessed by the exact solution of the partial differential equations: that is, the function e, Eq. (30), derived from the finite-difference solutions of the mass and momentum equations does not satisfy the finite-difference approximation of Eq. (28). Although the two approximations are the same in the theoretical limit as the mesh approaches zero, in practice the inclusion of terms of the

order of the truncation error alters the accuracy of the calculation and the computed value.

By casing the above concepts into the framework of averaged quantities and fluctuations from their averages, an insight can be achieved into the nature of the truncation error terms. Consider an averaging procedure such that the average of the sum is the sum of the averages, the average of the average is the average, and the average of a fluctuation is zero. The exact velocity can be written as the sum of the averaged velocity (doubled barred quantity) plus its fluctuation (primed quantity). Componentwise, we have

$$u = \bar{\bar{u}} + u' \qquad \text{and} \qquad v = \bar{\bar{v}} + v'.$$

The associated specific kinetic energy is

$$0.5(u^2 + v^2) = 0.5(\bar{\bar{u}}^2 + \bar{\bar{v}}^2) + 0.5(u'^2 + u'^2) + (\bar{\bar{u}}u' + \bar{\bar{v}}u'). \tag{37}$$

Using the properties of the averaging procedure, we can write the average of Eq. (37) as

$$\overline{\overline{0.5(u^2 + u^2)}} - 0.5(\bar{\bar{u}}^2 + \bar{\bar{v}}^2) = \overline{\overline{(0.5u'^2 + v'^2)}}. \tag{38}$$

The difference between the averaged exact specific kinetic energy and the specific kinetic energy of the averaged velocities is the averaged specific kinetic energy of the fluctuations which can be called the subgrid-scale specific kinetic energy. If we take the averaged values as the computed cell-centered values at the end of a single time step, then the first term on the left-hand side of Eq. (38) can be associated with the specific kinetic energy computed via the finite-difference approximation of Eq. (28) to a given order of accuracy and the second term can be associated with the specific kinetic energy computed via the cell-centered values of the mass and momentum. Consider, for example, the TPHASE approximation to the specific kinetic energy. If we multiply Eq. (33) by Δt and manipulate the result using the above associations, we have

$$0.5(\bar{\bar{u}}^2 + \bar{\bar{v}}^2) = \overline{\overline{0.5(u^2 + v^2)}} - \frac{\Delta t}{\rho^{n+1}}\{\text{truncation error terms}\}. \tag{39}$$

Comparing Eq. (38) with Eq. (39), we obtain

$$\overline{\overline{0.5(u'^2 + v'^2)}} = \frac{\Delta t}{\rho^{n+1}}\{\text{truncation error terms}\}. \tag{40}$$

From Eqs. (40) and (39), we see that the original formulation of HELP excludes the subgrid-scale kinetic energy. Accordingly, the direct calculation of the kinetic energy from Eq. (28) includes it.

The effect of these truncation error terms is not confined to the kinetic energy calculation but is directly translated to the internal energy calculation via Eq. (5). The accuracy of the internal energy calculation is of prime importance, since the pressure,

temperature, and strength properties of the material directly depend on the internal energy and not on either the total or kinetic energies. The dominant errors of the internal energy approximations in SPHASE can be seen by subtracting Eq. (34) from Eq. (15), in HPHASE by subtracting Eq. (35) from Eq. (20), and in TPHASE by subtracting Eq. (36) from Eq. (26). The results are for SPHASE,

$$\frac{\partial(\rho I)}{\partial t} - S_{xx}\frac{\partial u}{\partial x} - S_{xy}\left(\frac{\partial u}{\partial y} + \frac{\partial v}{\partial x}\right) - S_{yy}\frac{\partial v}{\partial y}$$
$$= -\frac{\Delta t}{2}\left[\frac{\partial^2(\rho I)}{\partial t^2} + \frac{1}{\rho}\left(\frac{\partial S_{xx}}{\partial x} + \frac{\partial S_{xy}}{\partial y}\right)^2 + \frac{1}{\rho}\left(\frac{\partial S_{xy}}{\partial x} + \frac{\partial S_{yy}}{\partial y}\right)^2\right]$$
$$+ O(\Delta t^2) + O(\Delta x^2) + O(\Delta y^2), \tag{41}$$

for HPHASE

$$\frac{\partial(\widetilde{\rho I})}{\partial t} + P\left(\frac{\partial \tilde{u}}{\partial x} + \frac{\partial \tilde{v}}{\partial y}\right) = \frac{-\Delta t}{2}\left[\frac{\partial^2(\widetilde{\rho I})}{\partial t^2} + \frac{1}{\rho}\left(\frac{\partial P}{\partial x}\right)^2 + \frac{1}{\rho}\left(\frac{\partial P}{\partial y}\right)^2\right]$$
$$+ O(\Delta t^2) + O(\Delta x^2) + O(\Delta y^2), \tag{42}$$

for TPHASE

$$\frac{\partial(\overline{\rho I})}{\partial t} + \frac{\partial(\rho \overline{Iu})}{\partial x} + \frac{\partial(\rho \overline{Iv})}{\partial y} = \frac{\Delta x}{2}\left\{\frac{\partial}{\partial x}\left[\bar{u}\frac{\partial(\rho \bar{I})}{\partial x}\right] + \rho\bar{u}\left[\left(\frac{\partial \bar{u}}{\partial x}\right)^2 + \left(\frac{\partial \bar{v}}{\partial x}\right)^2\right]\right\}$$
$$+ \frac{\Delta y}{2}\left\{\frac{\partial}{\partial y}\left[\bar{v}\frac{\partial(\rho \bar{I})}{\partial y}\right] + \rho\bar{v}\left[\left(\frac{\partial \bar{u}}{\partial y}\right)^2 + \left(\frac{\partial \bar{v}}{\partial y}\right)^2\right]\right\}$$
$$- \frac{\Delta t}{2}\left\{\frac{\partial^2(\overline{\rho I})}{\partial t^2} - 2\frac{\partial}{\partial x}\left(\rho \overline{Iu}\frac{\partial \bar{u}}{\partial x}\right) - 2\frac{\partial}{\partial y}\left(\rho \overline{Iv}\frac{\partial \bar{v}}{\partial y}\right)\right.$$
$$\left. + \bar{\rho}\left[\left(\bar{u}\frac{\partial \bar{u}}{\partial x} + \bar{v}\frac{\partial \bar{u}}{\partial y}\right)^2 + \left(\bar{u}\frac{\partial \bar{v}}{\partial x} + \bar{v}\frac{\partial \bar{v}}{\partial y}\right)^2\right]\right\}$$
$$+ O(\Delta t^2) + O(\Delta x^2) + O(\Delta y^2), \tag{43}$$

where we have assumed $\Delta x = \Delta y$ in order to simplify the TPHASE $O(\Delta t)$ term. The accuracy of the internal energy calculation depends primarily on the magnitude of the first-order terms. The larger these terms are, the less accurate is the calculation. The derivative of (ρI) plus positive terms which are a consequence of the truncation error terms in the kinetic energy calculation. These positive terms could be excluded from the kinetic energy calculation, and hence the internal energy calculation, without changing the order of the truncation error of the HELP algorithm. When the second time derivative of (ρI) is nonnegative, the SPHASE and HPHASE internal energy values are computed with less accuracy than would occur if these truncation error terms were excluded. A typical time history of the quantity (ρI) for a conical-shaped charge simulation (see Section IV) is given in Fig. 2. The curvature of this graph is

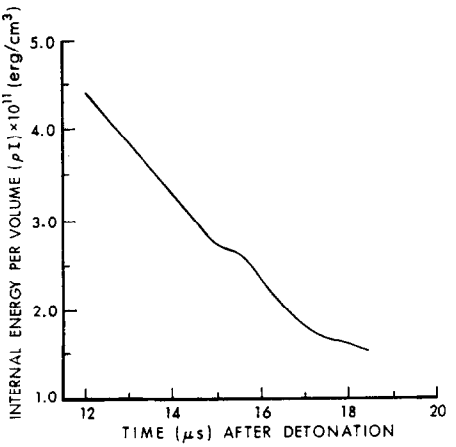

FIG. 2. Typical time history profile of the internal energy per volume in a conical-shaped charge calculation.

nonnegative except for a short interval corresponding to the stagnation region within a shaped charge. Thus, at least for significant portions of a shaped charge simulation, the internal energy calculation in SPHASE and HPHASE is less accurate because of the inclusion of the truncation error terms from the kinetic energy calculation. Furthermore, even if the curvature of (ρI) with respect to time was negative, the accuracy of the internal energy would be less, provided the terms associated with the truncation error terms from the kinetic energy calculation were much larger than the magnitude of the curvature of (ρI).

In the TPHASE calculation, each of the three first-order terms in Eq. (43) should be analyzed to ascertain the effects of the truncation error terms from the kinetic energy calculation (the squared terms in Eq. (43)) on the internal energy calculation. In shaped charge simulations, the $O(\Delta y)$ term dominates the $O(\Delta x)$ and $O(\Delta t)$ terms, since the velocity and direction of the rate of change is primarily in the y direction and since a fairly coarse spatial computing mesh must be used ($O(\Delta y) \simeq 10^{-2}$ versus $O(\Delta t) \simeq 10^{-8}$). Hence, we consider only the $O(\Delta y)$ term, which we rewrite as:

$$\frac{\partial \bar{v}}{\partial y}\frac{\partial(\rho \bar{I})}{\partial y} + \bar{v}\frac{\partial^2(\rho \bar{I})}{\partial y^2} + \rho \bar{v}\left[\left(\frac{\partial \bar{u}}{\partial y}\right)^2 + \left(\frac{\partial \bar{v}}{\partial y}\right)^2\right]. \tag{44}$$

Typical spatial profiles in shaped charge calculations of the quantities v and (ρI) along the axis of symmetry are given in Fig. 3. Since v is always positive and $\partial v/\partial y$, $\partial(\rho I)/\partial y$, and $\partial^2(\rho I)/\partial y^2$ are nonnegative throughout most of their variation, the sum of the first two terms is generally nonnegative. Consequently, since the third and fourth terms are always positive, the accuracy of the internal energy calculation is decreased. Thus, as was seen in the SPHASE and HPHASE approximations, the internal energy calculation for shaped charge calculations would generally be more accurate, if the truncation error terms from the kinetic energy calculation were excluded.

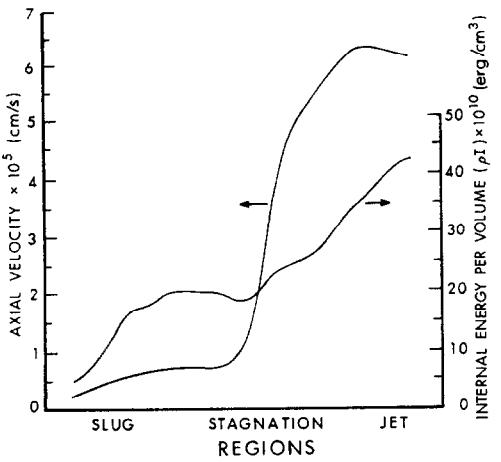

FIG. 3. Typical spatial profiles of the axial velocity and internal energy per volume in a conical-shaped charge calculation.

Another example of a flow in which the truncation error terms from the kinetic energy calculation would severely affect the internal energy calculation is in the expansion of perfect gas in a uniform pressure field. For a perfect gas, we have the relation $\rho I = P(\gamma - 1)^{-1}$ where the constant γ is the ratio of specific heats. Consequently, in a uniform pressure field, the quantities $\partial^2(\rho I)/\partial t^2$, $\partial(\rho I)/\partial x$, and $\partial(\rho I)/\partial y$ would be zero in Eqs. (41)–(43). If the truncation error terms from the kinetic energy calculation were excluded, the entire $O(\Delta t)$ term in SPHASE would be zero as well as the entire $O(\Delta x)$ and $O(\Delta y)$ terms in TPHASE. Thus, the internal energy approximations in SPHASE would be $O(\Delta t^2)$ and TPHASE $O(\Delta x^2)$ and $O(\Delta y^2)$. Consequently, the approximations achieve a higher order of accuracy when the extraneous terms are excluded.

In other applications, the order of magnitude and/or the algebraic signs of the first-order terms in Eqs. (41)–(43) must be analyzed in order to determine the effects of truncation error terms from the kinetic energy calculation on the accuracy of the internal energy calculation. In regions of large gradients, the magnitude of these truncation error terms can be large because of their quadratic dependence on the first spatial derivatives. Since limitations on running time and machine storage necessitate fairly coarse computing meshes for two-dimensional simulations, the truncation errors related to the finite size of the mesh cell are more likely to be important than those related to the time step. Thus, the $O(\Delta x)$ and $O(\Delta y)$ terms in Eq. (43) may dominate the truncation error. We shall see that this is the case in shaped charge calculations.

The inclusion of the truncation error terms in the kinetic energy calculation alters not only the computed values of the kinetic energy of a cell at each cycle but also the values of the internal energy. The coefficients of the Δt terms in Eqs. (31) and (32) are positive and increase the kinetic energy. For equal spatial meshes ($\Delta x = \Delta y$), the

entire first-order term in the TPHASE calculation is negative for Courant numbers less than a half and decreases the kinetic energy. The effects of the truncation error terms on the internal energy is reversed because of Eq. (5). The SPHASE and HPHASE terms decrease the internal energy and the TPHASE increases it. Thus, these terms can be interpreted as a transfer mechanism which is not modeled by the governing equations and which converts internal energy into kinetic energy and kinetic energy into internal energy. Consider, for example, the one-dimensional first-order energy approximation in TPHASE for motion in the x-direction. The only first-order term that the internal energy calculation includes is the positive term:

$$\frac{\rho\rho_{i-1}\bar{u}^l}{2\rho^{n+1}}(\Delta x - \bar{u}^r\,\Delta t)\left(\frac{\bar{u} - \bar{u}_{i-1}}{\Delta x}\right)^2. \tag{45}$$

Expanding expression (45) in a Taylor series about the cell center and the nth time level, we obtain

$$(\lambda - \lambda')\left[\frac{\partial u}{\partial x}\right]^2 \tag{46}$$

to the lowest order, where $\lambda = 0.5\rho u\Delta x$ and $\lambda' = +0.5\rho u^2\Delta t$. If $(\lambda - \lambda')$ were the coefficient of viscosity, then expression (46) would be identical to the viscosity term in the one-dimensional internal energy equation for a viscous fluid. Thus, the energy transfer mechanism in this case could be defined as an explicit artificial viscosity term, since it is explicitly included in the difference equation much like the implementation of the von Neumann and Richtmyer artificial dissipation scheme. Evans and Harlow[3] identified the term corresponding to $\lambda(\partial u/\partial x)^2$ in their one-dimensional analysis of the original PIC code. The term $\lambda'(\partial u/\partial x)^2$ is not included in their analysis, since they did not include the effect of time differencing. From expression (46), we see that the time discretization decreases the amount of kinetic energy converted to internal energy in TPHASE. This explicit type of artificial viscosity is confined only to the TPHASE energy calculation and is, in addition to the implicit artificial viscosity [6] (that type of artificial viscosity deduced from the neglected truncation error terms within an algorithm), already inherent in a first-order algorithm.

We have shown that the terms of the order of the truncation error which are included in the kinetic energy calculation decrease the accuracy of the internal energy calculation under certain circumstances. To determine the effects of omitting these terms in such a calculation, the HELP code was modified to allow a kinetic energy calculation which did not include the first-order terms in Eqs. (31)–(33). Consequently, the kinetic energy was not computed by the updated mass and momentum values but was considered a separate dependent variable. This kinetic energy for both pure and mixed cells was updated according to a direct finite differencing of Eq. (28) in a manner consistent with the other approximations and was stored in an array. This modified version required slightly less computing time than the original version, since all the quantities needed to compute a new kinetic energy value are already available from the mass and momentum calculations and future references to the kinetic energy are

simply retrievals. A natural alternative to the above approach is the calculation of the internal energy by a direct approximation of its partial differential Eq. (29). However, a stated purpose [1] for the current total energy version of HELP is the avoidance of free-surface pressure and velocity problems rising from a direct internal energy calculation. The desire to avoid past difficulties within HELP compelled us away from a direct internal energy formulation and to the retention of the total energy formulation with a modified kinetic energy calculation. This modified code, while still rigorously conserving total energy, will avoid the algorithmic interchanging of kinetic and internal energies which are not modeled by the partial differential equations. The results of this modified formulation are compared to those of the original version for typical HELP applications at the Ballistics Research Laboratory in the next section.

IV. Examples

The HELP code is used at the Ballistics Research Laboratory to simulate the detonation and jet formation of a shaped charge, an armor piercing warhead. We will consider an unconfined conical-shaped charge (see Fig. 4a). The actual warhead is obtained by rotating Fig. 4a about the axis of symmetry. The explosive is detonated and the detonation wave collapses the conical liner toward the axis of symmetry with a varying velocity. Sixteen microseconds after detonation, the liner consists of three parts (Fig. 4b): the uncollapsed liner, the low velocity large mass slug, and the high velocity small mass jet. By performing a Galilean transformation at the point where

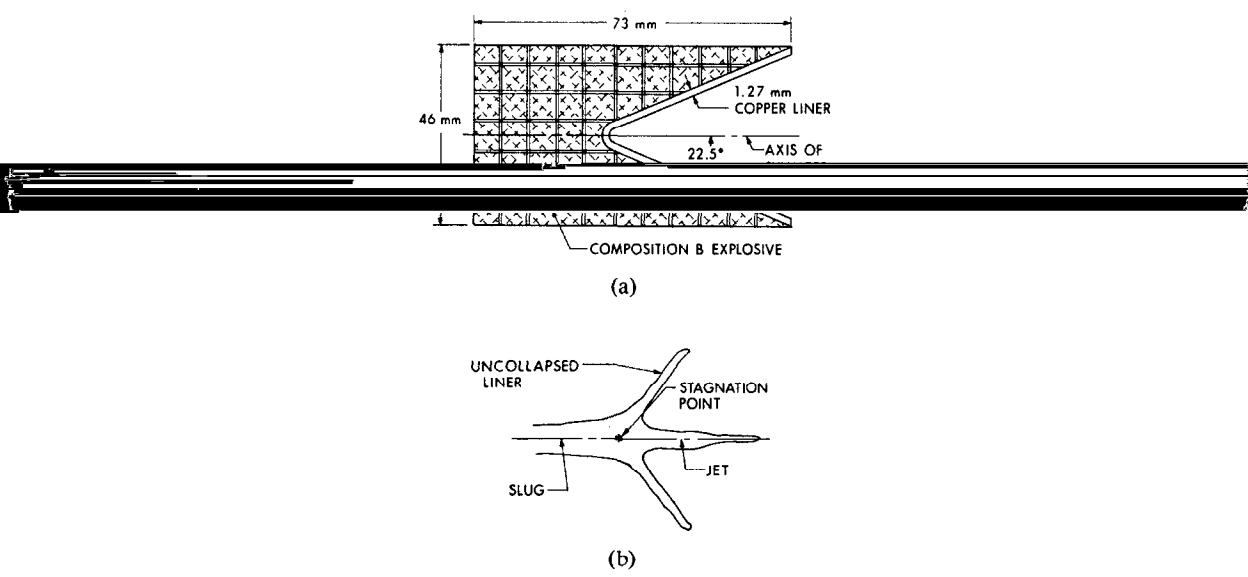

FIG. 4. (a) Initial conical-shaped charge configuration. (b) Copper configuration at 16 μs for conical-shaped charge.

an original ring of liner impinges on the axis of symmetry, a stagnation point in the flow can be shown to exist. This stagnation point divides the collapsed liner into the slug and jet. It is the jet which pierces the armor and is of prime concern to the shaped charge designer. By assuming that the liner can be modeled as an incompressible inviscid fluid under typical loading conditions, several researchers [7–9] have developed one-dimensional analytical or simple numerical models to determine the velocity field. However, when two-dimensional axisymmetric geometry, compressibility, strength, and thermodynamic effects are included, a full numerical simulation is necessary.

Since the preceding study was based on a truncation error analysis, a mesh refinement study is appropriate to the investigation of the effects of the truncation error terms on the accuracy of the computed specific internal energies. Because of the complexity of a full shaped charge simulation, a related model problem [7] is simulated in the mesh refinement study. An observer stationed at the stagnation point in Fig. 4b would find the uncollapsed liner moving toward him and separting into two parts (the slug and the jet). Consequently, a 2-cm-wide copper wedge traveling at 2×10^5 cm/s was simulated as it impinged on a perfectly reflective wall at 60° of obliquity. The wedge collapse was modeled with slab symmetry and the identical material constants used in a shaped charge calculation. The Tillotson equation of state [10] for copper was used. The coarse computational mesh was 30×100 cells ($\Delta x = \Delta y = 0.1$ cm) and the fine mesh was 60×200 cells ($\Delta x = \Delta y = 0.05$ cm). Both the original and modified version of the HELP code were run on a CDC 7600.

The results at 10 μs after the wedge first impacts the wall are shown in Figs. 5–7. Besides the specific internal energy, two other important quantities, the relative axial velocity (relative to the end of the slug portion) and density, are compared along the wall in the slug, stagnation, and jet regions. Qualitatively, the entire relative axial velocity and compression curves and the slug portion of the specific internal energy curve are similar among the mesh variations and version changes. However, the qualitative behavior of the jet's specific internal energy markedly differs between the two versions for either mesh. This is due to the increased gradients within the jet portion which drastically increase the magnitude of the truncation error terms from the kinetic energy calculation, and thus, the truncation error. Quantitative comparisons were made at three positions in Figs. 5–7: the slug end, the stagnation point (denoted by ↓), and the jet end. While the total deviation from the largest computed value at the three stations among the relative axial velocity and compression curves was less than 7% (except for 9.9% in the compression at the jet's end), the total deviation of the specific internal energy curve was 82.1, 26.4, and 63% at the jet, stagnation, and slug, respectively. The tremendous increase in the total deviation of the specific internal energy curve is due to the first-order terms included in the calculation of the kinetic energy. In fact, the deviation of the coarse mesh specific internal energy results from the fine mesh results, decreased by over 62% from the original version to the modified version. Consequently, one obtains much less variation in the specific internal energy values as one converges to the solution through a mesh refinement with the modified version. Figure 7 suggests that

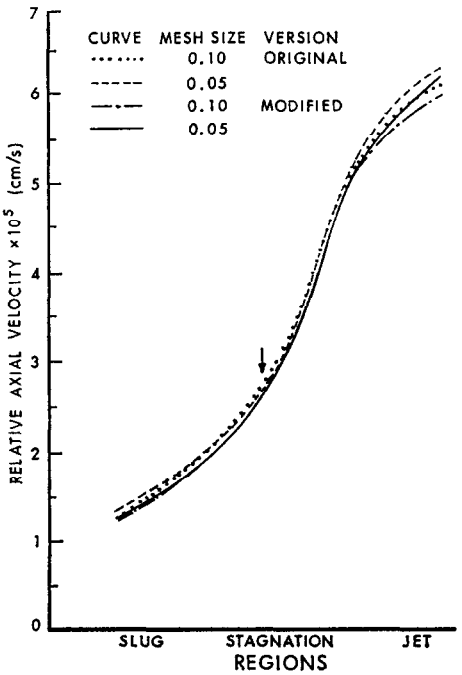

FIG. 5. Spatial profiles of the relative axial velocity at 10 μs along the wall for a copper wedge impact calculation.

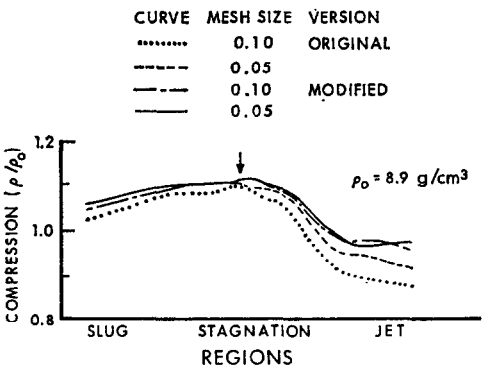

FIG. 6. Spatial profiles of the compression at 10 μs along the wall for a copper wedge impact calculation.

the specific internal energy values which are computed by the modified version and with the coarse mesh provide a better approximation to the exact values than those values computed by the original version with the fine mesh. This trend is also present in the compression curve. The results of Fig. 7 also show that for this type of problem, the truncation error terms in the kinetic energy calculation associated with TPHASE (Courant number of 0.4 is used) dominate those

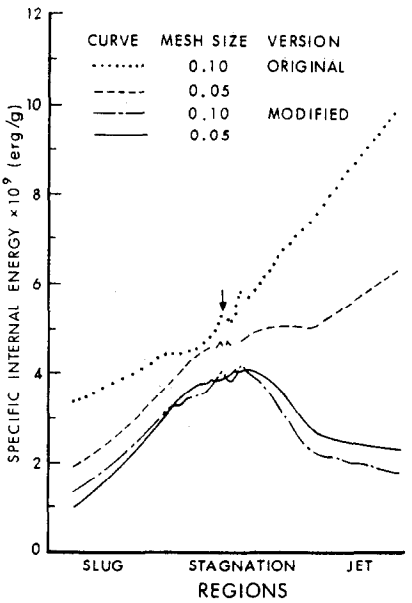

FIG. 7. Spatial profiles of the specific internal energies at 10 μs along the wall for a copper wedge impact calculation.

associated with SPHASE and HPHASE and cause the specific internal energy to be increased.

In order to further compare the original and modified versions of the HELP code, a conical-shaped charge with a copper liner and Composition B explosive (Fig. 4a,) was modeled in cylindrical coordinates and with identical material constants, initial conditions, code options, and grid structure. The computational mesh was 60 cells ($\Delta r = 0.052$ cm) by 187 cells ($\Delta z = 0.052$ cm). The initial state was quiescent: all properties zero except the standard values of the densities. The Jones–Wilkins–Lee equation of state [11] for the explosive and the Tillotson equation of state [10] for the copper were used. The calculations were performed on a CDC 7600.

In the original formulation, the specific internal energy of each cell in the jet is well above the value corresponding to incipient vaporization (13.8×10^9 erg/g) at 16 μs. Thus, the jet is characterized as a liquid–vapor jet. However, with the modified formulation, the specific internal energy of the same cells is generally below that for melt (5.3×10^9 erg/g) and a solid jet with several melted sections is predicted. See Fig. 8. The specific internal energy value corresponding to the melting point is a material property input value and that value corresponding to the incipient vaporization point is contained within the Tillotson equation of state. Although no actual temperature has been taken for this shaped charge, other experimental evidence [12] supports the conclusion that the jet is a solid. Thus, qualitative thermal agreement is achieved with the modified formulation. This comparison of the jet's internal energies shows that in the original formulation, the truncation error terms in the kinetic

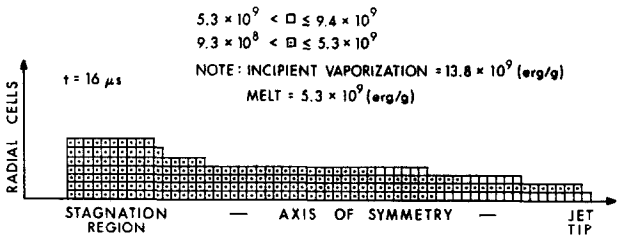

FIG. 8. Cell values of the specific internal energy (erg/g) of the copper jet computed by the modified formulation.

energy calculation associated with TPHASE (Courant number is 0.4) dominate those associated SPHASE and HPHASE. In fact, throughout the flow field, the original formulation gave higher values of the internal energy than the modified formulation. A comparison of the magnitude of the computed specific internal energies along the axis of symmetry between the two formulations is given in Fig. 9. The modified code predicts up to an 88% decrease in the specific internal energy of the original code. Such major changes in the internal energy will drastically affect the material properties of the jet, such as its strength, ductility, and cohesion. Two other quantities important to the warhead designers are the density and axial velocity. Figures 10 and 11 show comparisons of the compression and axial velocity of the jet along the axis of symmetry. The jet density of the modified code is approximately 10% higher than the original. Near the stagnation region, the modified formulation gives an improved result: a compression ($\rho > \rho_0$) of the copper. The density discontinuity near the jet tip which may not be physical is of smaller magnitude in the modified version. The axial velocities (Fig. 11) are virtually identical except near the jet tip where the physical

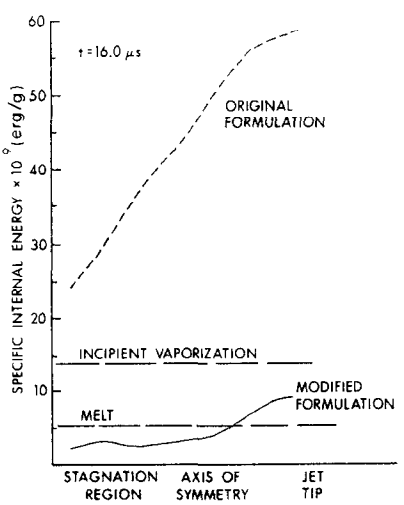

FIG. 9. Comparison of the jet's specific internal energy along the axis of symmetry at 16 μs.

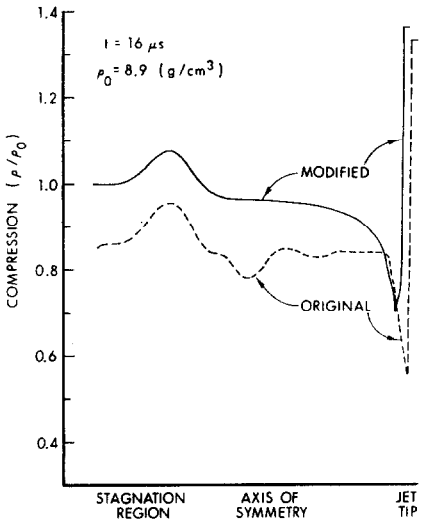

FIG. 10. Comparison of the jet's compression along the axis of symmetry at 16 μs.

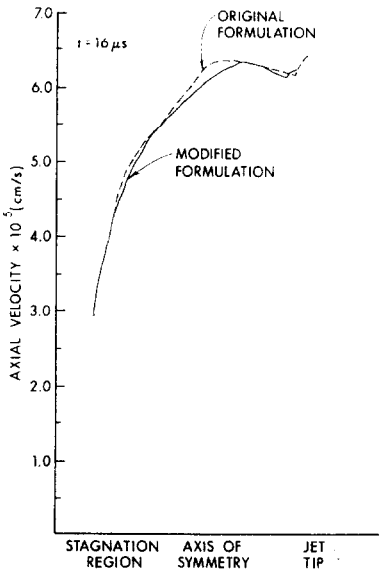

FIG. 11. Comparison of the jet's axial velocity along the axis of symmetry at 16 μs.

inverse velocity gradients are present but have small magnitudes. The larger axial

computational cells). The relative jet tip velocity (jet tip velocity minus slug tail velocity) of 6.02×10^5 cm/s is 7.9% lower than that indicated by experimental flash radiographs. The discrepancies between the density and axial velocities would be

much greater if the original version did not have an artificial cutoff value (13.8×10^9 erg/g) for the specific internal energy in the equation of state for the liner material. Since the cell values of the jet's specific internal energy are well above the cutoff value in the original formulation, the pressure, velocity, total energy, and mass do not include the effects of the computed high internal energies.

V. Summary

We have shown by a truncation error analysis that terms of the order of the truncation error in the HELP algorithm are included in the kinetic energy calculation. In the original HELP code, the updated values of kinetic energy were computed as consequences of the updated mass and momentum values. This value is shown to deviate from that computed directly by a first-order approximation of the kinetic energy equation by first-order terms which depend quadratically on the spatial derivatives of the velocity, pressure, and elements of the deviator stress tensor. These truncation error terms can severely alter the related internal energy calculation. The effect of these truncation error terms from the kinetic energy calculation on the accuracy of the internal energy is problem dependent and the criteria for such a determination is given in terms of the explicitly calculated truncation error terms for the specific internal energy. A method was suggested to avoid these terms within the confines of the basic HELP algorithm. Although in certain computations these truncation error terms from the kinetic energy calculation may remain negligible, in others they can be significant and produce spurious results. A case in point has been cited and illustrated by applications to problems in warhead mechanics. A mesh refinement study for a copper wedge impacting a perfectly reflective wall was made. The results show tremendous deviations in the internal energy values as the mesh size decreases, while other quantities show relatively little deviations. In the modified formulation, significantly smaller deviations in the internal energy values and, consequently, a more consistent deviation with the other quantities are observed. Drastic improvements in the internal energy values are also seen in conical-shaped charge calculations. In these simulations, the internal energies which are compatible with experimental results are obtained for the first time with the modified formulation. Furthermore, the upper bound on the specific internal energy in the Tillotson equation of state for the liner material has been removed in the modified formulation. Now the specific internal energy value used in the pressure calculation is always the value calculated by the algorithm.

In the TPHASE section of the original HELP algorithm the truncation error terms from the kinetic energy calculation are identified with an explicit artificial viscosity in the internal energy calculation. Consequently, the modified formulation may require implementation of the artificial viscosity option available in cases where the original formulation did not.

A noteworthy feature of the analysis and modification is that it is directly relevant to codes other than HELP. In fact, any code with a HELP-type algorithm can be

erroneously affected by truncation error terms in the kinetic energy calculation. In particular, the same unphysical internal energies in the jet are computed by the HULL code.

ACKNOWLEDGMENT

The author wishes to thank the reviewers for their helpful suggestions in the preparation of this paper.

REFERENCES

1. L. J. HAGEMAN, D. E. WILKINS, R. T. SEDGWICK, AND J. L. WADDEL, Systems Science and Software Report SSS-R-75-2654, 1975.
2. M. A. FRY *et al.*, Air Force Weapons Laboratory Report AFWL-TR-76-183, 1976.
3. M. W. EVANS AND F. H. HARLOW, Los Alamos Scientific Report LA-2139, 1957.
4. F. H. HARLOW, The particle-in-cell computing method for fluid dynamics, in "Methods in Computational Physics" (B. Alder, S. Fernback and M. Rothenberg, Eds.), Academic Press, New York, 1964.
5. F. H. HARLOW, The particle-in-cell method for numerical solution of problems in fluid dynamics, *in* "Proceedings of Symposia in Applied Mathematics" (N. Metropolis, J. Todd, A. Tank, and C. Tompkins, Eds.), Vol. XV, Amer. Math. Soc., Providence, R. I., 1963.
6. P. J. ROACHE, "Computational Fluid Dynamics," Chap. V, Hermosa, Albuquerque, 1976.
7. G. BIRKHOFF, D. P. MACDOUGALL, E. M. PUGH, AND G. TAYLOR, *J. Appl. Phys.* **19** (1948), 563.
8. E. M. PUGH, R. J. EICHELBERGER, AND N. ROSTOKER, *J. Appl. Phys.* **23** (1952), 532.
9. A. R. KIWAN AND H. WISNIEWSKI, BRL Report No. 1620, 1972.
10. J. H. TILLOTSON, General Atomic Report GA-3216, 1962.
11. E. LEE, M. FINGER, AND W. COLLINS, Lawrence Livermore Laboratory Report UCID-16189, 1973.
12. W. G. VON HOLLE AND J. J. TRIMBLE, Shape charge temperature measurement, *in* "Proceedings of the Sixth Symposium on Detonation," ACR-221, Office of Naval Research, Arlington, VA, 1976.